

# ULTRA-HIGH-PERFORMANCE FIBRE-REINFORCED CONCRETE UNDER HIGH-VELOCITY PROJECTILE IMPACT. PART I. EXPERIMENTS

SEBASTJAN KRAVANJA<sup>a</sup>, RADOSLAV SOVJÁK<sup>b,\*</sup>

<sup>a</sup> Faculty of Civil and Geodetic Engineering, University of Ljubljana, Jamova cesta 2, Ljubljana 1000, Slovenia

<sup>b</sup> Faculty of Civil Engineering, Czech Technical University in Prague, Thákurova 7, 166 29 Prague 6, Czech Republic

\* corresponding author: [sovjak@fsv.cvut.cz](mailto:sovjak@fsv.cvut.cz)

**ABSTRACT.** A series of cratering experiments were performed where the response of the Ultra-High-Performance Fibre-Reinforced Concretes with various fibre volume fractions to the high-velocity projectile impact loading was investigated. It was found that the increment of the fibre volumetric fraction did not have a significant influence on the depth of the penetration, but it was very effective in reducing the crater area and volume.

**KEYWORDS:** projectile impact; UHPFRC; depth of penetration; mechanical properties; shear crack resistance.

## 1. INTRODUCTION

As the occurrence of unexpected events is ever increasing in today's society, a primary loading type that needs to be addressed is the localized impact of projectiles. In a broad sense, the projectile impact might be understood as a fragment generated from a high-speed rotating machine, explosion generated fragment, and last but not least a projectile generated from a direct armed attack. The projectile impact can be considered as a high strain-rate loading caused by an object travelling with high speed and having a relatively low weight. This kind of loading is characterized by its rapid increase in the release of energy in a very short time. Several damage mechanisms are activated at once during the projectile penetration, such as compaction, compression with confining pressure and tension cracking. The complexity is further increased since the strain rate effect is different for each mechanism [1]. To simulate the effects of possible damage by the projectile impact, a series of small firearms tests with live ammunition was carried out.

Several authors suggested that structures are required to withstand impact loads generated by projectiles and in case of the plant-internal accidents [2, 3]. A typical case of this phenomenon is a fracture of the rotary machine, which could occur in turbine missiles, which are projectiles travelling at high velocities [4]. Perforating the wall of the turbine may result in a severe damage to the facilities and endangering the safety of the personnel [5].

Concrete is commonly used as an engineering solution due to its ability to withstand impact and point loads. A further potential expansion in the use of concrete has been indicated by the development of Ultra-High-Performance Fibre-Reinforced Concrete

(UHPFRC). For instance, Riedel et al. [6] implied that the UHPFRC is potentially suitable for improved protective structural elements. Consistently, other researchers also noted that the UHPFRC is a feasible solution for protective structures due to its enhanced mechanical properties and impact resistance [7, 8].

Impact resistance of the UHPFRC was evaluated through a three main damage degrees, such as depth of the penetration and area and volume of the impact crater. Beside the measurements of the impact resistance, several mechanical properties of the UHPFRC were determined for the means of the study of correlation to damage degrees.

In addition to experimental results, a shear crack analysis on cut through samples through the point of the deepest penetration was performed. The goal was to characterize the shear crack impact resistance of the UHPFRC for various fibre volume fractions.

## 2. MATERIAL AND METHODS

### 2.1. UHPFRC

The concrete base mixture was made using a low water-to-binder ratio and contained common high-performance concrete ingredients, such as ordinary Portland cement binder, silica fume, superfine aggregates with a maximal size of a grain of 1.2 mm, superplasticizer (high-range water reducer) in powder form, water and anti-foaming agent [9]. For the fibre reinforcement of the specimens, straight, discrete, high-strength steel fibres were used with a length and diameter of 14 mm and 0.13 mm, respectively. The material of the fibres had the density of 7850 kg/m<sup>3</sup>, the tensile strength of 2800 MPa and elastic modulus of 200 GPa.

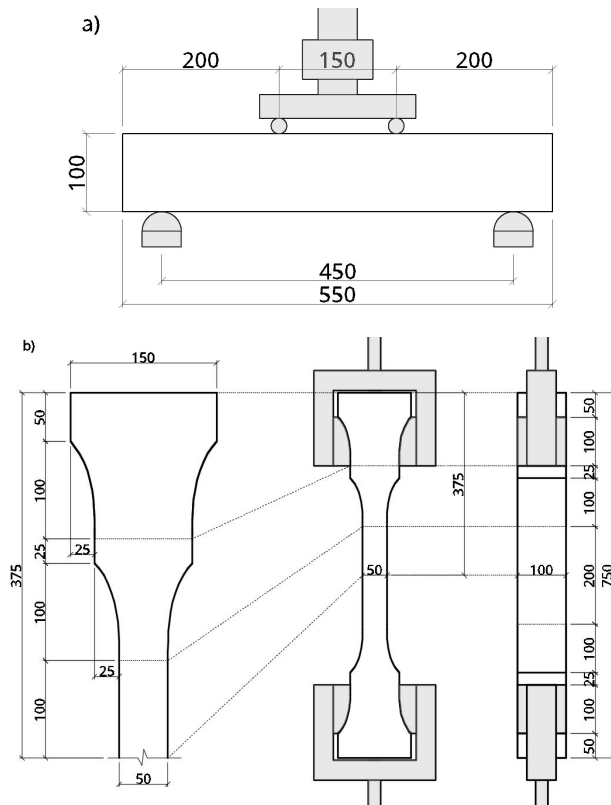


FIGURE 1. Experimental set-up for determination of tensile mechanical properties of UHPFRC. a) Prism used for 4-point flexural strength test (i.e. modulus of rupture). b) Dog-bone shaped specimen used for the direct tensile strength test with clothoid transitions.

Five different fibre volumetric fractions were set with gradually enlarging increments by the doubling geometric sequence in the form of  $V_{f,i} = 0.125(2^{i-1})$  for  $1 \leq i \leq 5$  which yielded:  $V_{f,1} = 0.125\%$ ,  $V_{f,2} = 0.25\%$ ,  $V_{f,3} = 0.5\%$ ,  $V_{f,4} = 1\%$  and  $V_{f,5} = 2\%$ . In addition, the plain mixture specimens without fibre addition were also cast as a control and comparison samples labelled for the case where  $i = 0$  as  $V_{f,0} = 0\%$ . The plain mixture specimen is also referred in the text as an ultra-high-performance concrete (UHPC).

## 2.2. MECHANICAL PROPERTIES

Mechanical properties including unconfined compressive strength, flexural tensile strength (modulus of rupture) and direct tensile strength were investigated in the framework of the experimental part of the study. At least six specimens were tested for every mechanical property in the framework of the individual fibre volumetric content considered in this study.

Compressive strength was determined on cubes ( $100 \times 100 \times 100$  mm) by monotonic increments of the load by  $0.6$  MPa/s. A modulus of rupture was determined on prisms in a four-point bending configuration without a notch (Fig. 1a). The prisms were  $100 \times 100 \times 550$  mm in size and the clear span was  $450$  mm. The constant moment region regarding the four-point bending configuration was  $150$  mm. The

test was a deformation controlled and the loading rate was  $0.05$  mm/min. A pair of the LVDT (linear variable differential transformer) sensors was attached to the beam in the mid-span.

Flexural toughness factor ( $FT_{\delta}$ ) was determined according to a method for testing flexural strength and flexural toughness of a fibre reinforced concrete [10, 11]. Flexural toughness factor was calculated through an area of the load-displacement diagram of the prism constructed of the UHPFRC up to a load point deflection of span/150 [12].

Direct tensile strength was determined by using a dog-bone shaped specimen with a central part  $200$  mm in length and a reduced cross-section of  $50 \times 100$  mm. The total length of the dog-bone specimen was  $750$  mm and narrowing of its cross-section was done by means of clothoids  $100$  mm in length and  $25$  mm in height (Fig. 1b). The loading was deformation controlled with the loading rate set to  $0.05$  mm/min.

Furthermore, two additional mechanical properties were calculated. Wille et al. [13] introduced the variable  $g$  that is defined as the energy absorbing capacity prior to a tension softening and variable  $G$  that is defined as the fracture energy dissipated per crack surface. Energy absorbing capacity ( $g$ ) and fracture energy ( $G$ ) under direct tension were gained from the stress-strain diagram and load-total crack width diagram, respectively. The strain of the specimen under a direct tension was measured by using a pair of strain gauges  $50$  mm in length that was glued on the sides of the dog-bone specimen in its reduced cross-section. After the crack localization, the total crack width was measured using 4 inductive sensors that were placed over the reduced cross-section of the dog-bone specimen. The mechanical properties of the resulting mixture are listed in Table 1.

## 2.3. IMPACT TESTING

In total, 38 specimens, which all had the same designed dimensions of a cube ( $200 \times 200 \times 200$  mm), were cast and tested. Six specimens for each fibre volumetric content and plain concrete mixture were made; except for the  $2\%$  fibre content specimens, for which eight specimens were made, considering that was established as the optimal amount of fibres regarding the previous research [14, 15].

The impact test was conducted using a semi-automatic rifle with calibre  $7.62 \times 39$  mm and two types of ogive-nosed projectiles (Fig. 2). The deformable projectiles had a full-metal jacket and a soft-lead core (FMJ-SLC or SLC), while the non-deformable projectiles had a mild-steel core with a smaller lead tip (FMJ-MSL or MSL). Both types of projectiles had a mass of  $8.04$  g and the outer diameter of  $7.92$  mm. The diameter of the core of the MSL projectile and SLC projectile was  $5.68$  mm and  $6.32$  mm, respectively.

In the research by Sovják et al. [14] with the same type of projectiles impacting UHPFRC plates with  $50$  mm and  $45$  mm thicknesses, it was found out that

Fibre volume fraction (%)	plain mixture	0.125	0.25	0.5	1	2
Cube compressive strength (MPa)	111	118	131	133	134	144
Modulus of rupture (MPa)	6.30	7.07	7.76	10.3	20.3	26.1
Flexural toughness factor (MPa)	0.07	2.66	5.37	8.88	17.5	20.7
Direct tensile strength (MPa)	3.54	3.58	3.60	3.83	5.05	6.52
Energy abs. capacity (kJ/m <sup>3</sup> )	0.170	0.171	0.215	0.229	0.303	1.270
Fracture energy (kJ/m <sup>2</sup> )	0.10	5.42	6.08	10.3	12.7	17.7
Bulk density (kg/m <sup>3</sup> )	2346	2355	2358	2365	2381	2421

TABLE 1. Mechanical properties of the resulting UHPFRC mixture with various fibre volume fractions.

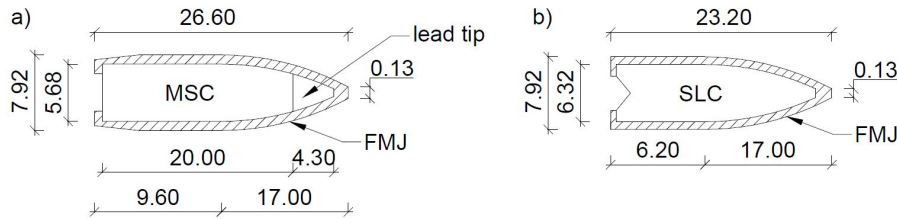


FIGURE 2. Projectiles used in the framework of this study and their dimensions in millimetres: a) full-metal jacket with the mild-steel core (FMJ-MS), b) full-metal jacket with the soft-lead core (FMJ-SLC).

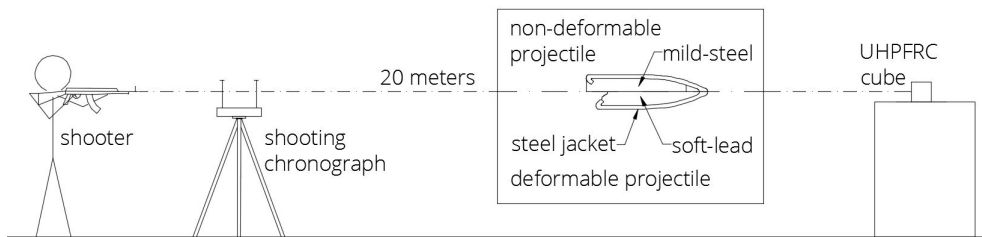


FIGURE 3. Experimental set-up of cratering experiments induced by two various projectiles on UHPFRC semi-infinite targets.

the steel jacket was separated during the penetration process and rebounded from the target. From the experimental observations, it was concluded that the diameter, which controls the penetration process, is the diameter of the core of the projectile ( $d_c$ ). In addition, no pith or yaw angles were noted from the records from the high-speed camera and it was concluded that a normal penetration occurred at all times.

The influence of the shape of the projectile head can be considered with the nose shape factor. The latter can be determined by the use of the ratio between the length of the projectile head and projectile diameter or with the use of Calibre Radius Head (CRH). CRH is a factor of projectile head sharpness and it is defined as a ratio between the projectile head radius of curvature  $R$  and projectile diameter  $d$  [16]:

$$CRH = \frac{R}{d}$$

Higher values of the CRH are implying sharper projectile's head and larger pressure at the target which result in a deeper total penetration depth. The calibre radius head of both types of projectiles was calculated based on the whole projectile diameter  $d$  and core diameter  $d_c$  (Table 2).

	FMJ-MS	FMJ-SLC
<b>External diameter</b> (mm)	7.92	7.92
<b>Core diameter</b> (mm)	5.68	6.32
<b>Total length</b> (mm)	26.60	23.20
<b>Jacket mass</b> (g)	4.15	2.78
<b>Core mass</b> (g)	3.65	5.26
<b>Tip mass</b> (g)	0.24	–
<b>Total mass</b> (g)	8.04	8.04
<b>Head radius of curvature <math>R</math></b>	28	31
<b>CRH(<math>d</math>)</b>	3.54	3.91
<b>CRH(<math>d_c</math>)</b>	4.93	4.91

TABLE 2. Non-deformable and deformable projectile geometrical and mass properties.

The average muzzle velocity for MSC and SLC projectiles was 710 m/s, while all the velocities were within the range of  $710 \pm 20$  m/s. The projectiles were fired from 20 m distance to the targets and hit them perpendicularly in the approximate centre of the proximal face under normal penetration (Fig. 3). The objective of the experimental part of this study was to investigate whether the increment in the fibre

Vf (%)	DOP (mm)	Area (cm <sup>2</sup> )	Volume (cm <sup>3</sup> )	Equivalent diameter (mm)	Cone failure angle (°)
0	36.41	84.70	–	101.7	26.83
0.125	35.78	50.58	30.33	84.38	33.42
0.25	35.72	37.53	23.17	72.17	39.75
0.5	35.13	21.97	14.50	64.18	47.08
1	33.37	24.48	15.67	63.10	46.17
2	31.43	18.99	11.50	54.83	51.81

TABLE 3. Average values for all measured or calculated damage degrees for FMJ-MSJ projectile impact.

Vf (%)	DOP (mm)	Area (cm <sup>2</sup> )	Volume (cm <sup>3</sup> )	Equivalent diameter (mm)	Cone failure angle (°)
0	20.59	114.4	96.33	114.8	22.33
0.125	19.61	40.87	25.33	74.63	35.42
0.25	18.80	39.71	24.00	74.08	40.75
0.5	20.46	30.12	20.00	68.55	47.58
1	20.09	33.20	20.67	73.49	41.83
2	20.04	21.12	13.88	57.22	46.31

TABLE 4. Average values for all measured or calculated damage degrees for FMJ-SLC projectile impact.

volumetric fraction within the concrete largely affects the damage intensity by measuring the dimensions of the crater made by the aforementioned impact. After the impact test, three main damage degrees were accurately measured, such as depth of penetration, crater area and crater volume, in order to quantitatively evaluate the difference in the damage resistance by enlarging the fibre volume fraction increment.

The impact velocity was determined from the measured muzzle velocity by using a shooting chronograph. The  $7.62 \times 39$  AK-47 (Kalashnikov) projectile with a mass of 8.04 grams is defined by Kneubuehl [17] to have the muzzle velocity 710 m/s and within 20 meters the velocity of the projectile is supposed to decrease to 688 m/s. Thus, all muzzle velocities measured in the framework of this study were reduced by 22 m/s, which yielded the actual impact velocity.

#### 2.4. SHEAR CRACK ANALYSIS

The analysis of shear cracks, produced by the projectile impact of both types was conducted on slices with a width of 10 mm, which were cut longitudinally through the target at the point of the maximum penetration depth. Cracks appeared in all of the samples; however, the intensity of the cracking was obviously decreasing with an increment of the fibre volumetric fraction. The intention was to quantitatively assess the crack impact resistance with respect to the fibre volumetric content increment. Shear crack angles and dimensions of cracks were measured using a ruler, microscope and CAD software. The crack impact resistance was evaluated through newly proposed factors of the impact resistance of brittle concrete composites reinforced with various fibres. Total shear crack lengths  $l_c$  and total depth of shear cracks  $z_c$  in each

specimen were measured and the number of major cracks  $n_c$  in each specimen was recorded. Shear crack widths were measured using a microscope (scale of 10  $\mu$ m).

The resistance against a shear crack propagation under the projectile impact was quantitatively evaluated through the use of the ultimate crack resistance factor  $R_u$ , recommended by Kankam [18] and revised by Alhasanat and Al Qadi [19]:

$$R_u = \frac{n_i E_k}{l_c z_c w_c},$$

where  $n_i$  is a number of blows,  $E_k$  impact (impulse) kinetic energy,  $l_c$  total length of all cracks,  $z_c$  maximum depth of the cracks and  $w_c$  maximum crack width, emerged due to the projectile impact.

Additionally, with the means of an efficient comparison with other composites or materials with different compressive strengths, the non-dimensional impact crack resistance ratio  $C_r$  was defined as a ratio between the ultimate crack resistance factor and unconfined compressive strength of the tested material:

$$C_r = \frac{R_u}{f'_c}.$$

### 3. RESULTS FOR THE CRATERING EXPERIMENTS

Numerical values of the experimental research are summarized in the (Tables 3 and 4). In all of the cases, the DOP was less than 38 mm, which is less than 1/5 of the target thickness, reaffirming the supposition of the semi-infinite target. In the cases of MSJ projectiles that impacted on the plain mixture specimens, an

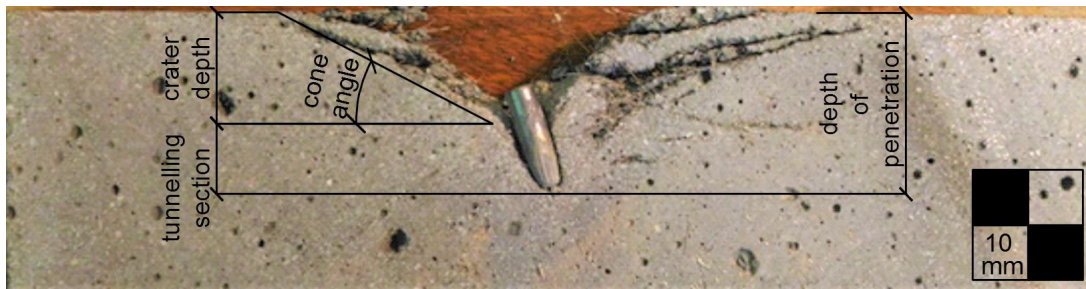


FIGURE 4. FMJ-MSJ projectile core (5.68 mm in diameter) penetrated into the sample 2.0 % FMJ-MSJ (the core was found rebounded from the target and inserted back in for presentation purposes).

intense shattering and fragmentation occurred in all three targets, whereas in the case of the SLC projectiles the less intense shattering occurred in two targets, while the third one remained in one piece. In all other specimens impacted by MSC projectiles, two parts of the impact crater appeared – the front crater (the spalling part) and the tunnelling part (Fig. 4). The tunnelling part of the crater slightly deviated from the straight trajectory, i.e. the so-called J-hook appeared during a cylindrical penetration. The MSC cores rebounded from the target and the non-deformed core was separated from the steel jacket during the penetration process. In the case of the SLC projectiles impact, only the spalling part emerged, while the soft lead core was completely destroyed during the impact.

The J-hook trajectory that was observed in the specimens under the MSC impact appeared as a change of the course during the penetration process due to the separation of the steel jacket and also by the anisotropic fracture process in concrete [1]. Other authors suggested that the projectile trajectory may deviate from a straight line during penetration due to the occurrence of instabilities or due to variable mechanical properties of the target [14, 16].

### 3.1. CORRELATION OF DAMAGE DEGREES TO MECHANICAL PROPERTIES

In recent years, doubts about the suitability of the use of concrete unconfined compressive strength as a parameter of a mechanical property of the target in prediction models have appeared. It is known that a vast majority of empirical and semi-analytical prediction models are derived on the basis of the general assumption that the depth of the penetration or volume of the crater is inversely proportional to the square root of the unconfined compressive strength of the tested concrete.

The concrete's unconfined compressive strength is worldwide used as the main classification parameter of concretes. As such, it is also set as an essential independent controlling variable in a vast majority of the impact prediction models. It is also known that the concrete compressive strength depends on specimen's geometry, cure time and above all, mix composition, whereas the latter differs substantially between normal strength concretes and high perfor-

mance concretes. Yankelevsky [20] is implying that since the increase in strength due to the variation of the concrete mix leads to a decreased porosity that affects the material compressibility and impact resistance, any smooth continuous function relating concrete compressive strength to impact damage parameters is an improper description of the concrete response to impact loading.

The basic correlation between the depth of the penetration or crater volume and inverse value of square root of unconfined compressive strength, on which the majority of models are derived, suggests that every concrete with the same unconfined strength exhibits an identical resistance to the impact penetration. It is known that the response of a concrete material to impact loading is conditioned on other concrete parameters as well, such as type, shape and size of aggregate, granulometric composition, additives, fibres type and volumetric content and so on, which can in different combinations result in a similar unconfined compressive strength but different impact resistance [20].

Yankelevsky is suggesting that this relationship supposition lacks physical meaning and seems to be arbitrarily predetermined. In order to test this hypothesis and furthermore assess the recent findings, a statistical evaluation of the correlation between three main damage degrees and tested mechanical properties has been conducted. Correlation coefficients between each of these quantities have been calculated and compared between values for each projectile type separately (Table 5).

It was already shown that in general, damage degrees' values are decreasing whereas mechanical strengths are increasing with an increment of the fibre volumetric fraction. It can be seen that in the case of the MSC projectile impact, the correlation coefficients are much larger than in the case of SLC projectile impact, especially in the case of the DOP. It can be also seen that the DOP in the MSC case is more correlated to tensile and flexural strength than unconfined compressive strength, whereas it is also strongly correlated to fracture energy, which is based on the direct tensile test. However, the crater area and crater volume are more correlated to the unconfined compressive strength in both projectile cases.

	FMJ-MSC			FMJ-SLC		
	DOP	Area	Volume	DOP	Area	Volume
$f'_c$	0.84	0.93	0.93	0.15	0.83	0.80
$\sqrt{f'_c}$	0.83	0.94	0.93	0.16	0.84	0.80
$f_t$	0.99	0.59	0.72	0.16	0.49	0.44
$\sqrt{f_t}$	0.99	0.61	0.73	0.17	0.50	0.45
$FT_\delta$	0.97	0.81	0.85	0.10	0.68	0.63
MOR	0.99	0.67	0.77	0.17	0.55	0.50
$g$	0.89	0.48	0.62	0.08	0.42	0.36
$G$	0.94	0.90	0.88	0.04	0.81	0.77

TABLE 5. Correlation coefficients for the dependency of damage degrees to mechanical properties of the tested UHPFRC.

$V_f$ (%)	FMJ-MSC			FMJ-SLC		
	$z_c$ (mm)	$l_c$ (mm)	$n_c$ (-)	$z_c$ (mm)	$l_c$ (mm)	$n_c$ (-)
0	141	—	—	113	353	5
0.125	90	430	6	97	232	6
0.25	72	370	6	60	175	5
0.5	79	269	6	66	135	4
1	68	110	4	40	84	3
2	52	88	3	20	58	3

TABLE 6. Crack dimensions.

$V_f$ (%)	FMJ-MSC			FMJ-SLC		
	$E_k$ (J)	$R_u$ (N/mm <sup>2</sup> )	$C_r$ (-)	$E_k$ (J)	$R_u$ (N/mm <sup>2</sup> )	$C_r$ (-)
0	1813.6	—	—	1966.0	49.3	0.4
0.125	1915.8	123.8	1.1	1838.9	204.3	1.7
0.25	1913.9	179.6	1.4	1878.9	447.4	3.4
0.5	1873.5	220.4	1.7	1868.0	524.1	3.9
1	1878.9	628.0	4.7	1893.6	1409.0	10.5
2	1905.6	1041.1	7.2	1880.8	4053.4	28.2

TABLE 7. Impact kinetic energy  $E_k$ , ultimate crack resistance factor  $R_u$ , impact crack resistance ratio  $C_r$ .

This is, however, in conflict with previous studies [21] showing that the tensile strength, strain softening, fracture energy, and strain-rate effect on the tensile strength in the prediction model are crucial for the dimensions of the crater area and volume. The reason for this may be attributed to the shallow penetration in these experiments where the depth of the penetration was no more than two times of the projectiles' length. As the tensile strength is crucial for the crater depth, the DOP is sensitive to the tensile strength in the shallow penetration where the crater depth is more than half of the DOP.

Furthermore, it should be noted that the compressive strength, tensile strength and flexural strength do not affect only the DOP. During the penetration process, the concrete material surrounding the projectile is subjected to a high-intensity triaxial stress state that can be described by the shear failure surface of concrete that must be determined by a large amount data of triaxial stress state, while the unconfined compressive or tensile strength is only a uniaxial stress state [21]. In addition, the volume change of concrete occurs during the penetration, thus the equation of state that is used to describe the relationship between pressure and volumetric strain plays an important role.

### 3.2. SHEAR CRACK RESISTANCE

For the FMJ-MSC projectile impact, the average shear crack width value was 0.16 mm, while for the FMJ-

SLC, it was 0.12 mm. In order to estimate the ultimate impact crack resistance factor, the maximal width was estimated for both type of projectiles for the UHPFRC as  $w_{c,max,UHPFRC} = 0.4$  mm. In the case of the FMJ-SLC projectile impact on plain UHPC specimens, where the target was not defragmented, the maximal width was estimated as  $w_{c,max,UHPC} = 1.0$  mm, in the case of the FMJ-MSC projectile impact on plain UHPC specimens, all the targets were defragmented and no additional cracks appeared in the remaining segment of the target (Table 6).

With the measured data and calculated impact kinetic energies  $E_k$  from estimated impact velocities, the ultimate impact crack resistance factor  $R_u$  and crack resistance ratio  $C_r$  were calculated (Table 7).

It can be observed that with the increment of the fibre volumetric fraction, the ultimate crack resistance factor of the UHPFRC is increasing with a constant trend (Fig. 5). The crack resistance increases with larger increments in the case of the SLC projectiles impact, since a lot of the impact energy is already dissipated with the significant deformation of the deformable lead core.

It can be concluded, that the fibre volumetric fraction increment up to 2% is efficient in providing the impact crack resistance to the otherwise brittle high-performance concrete matrix. This property is essential in providing further impact resistance against additional projectile impacts.

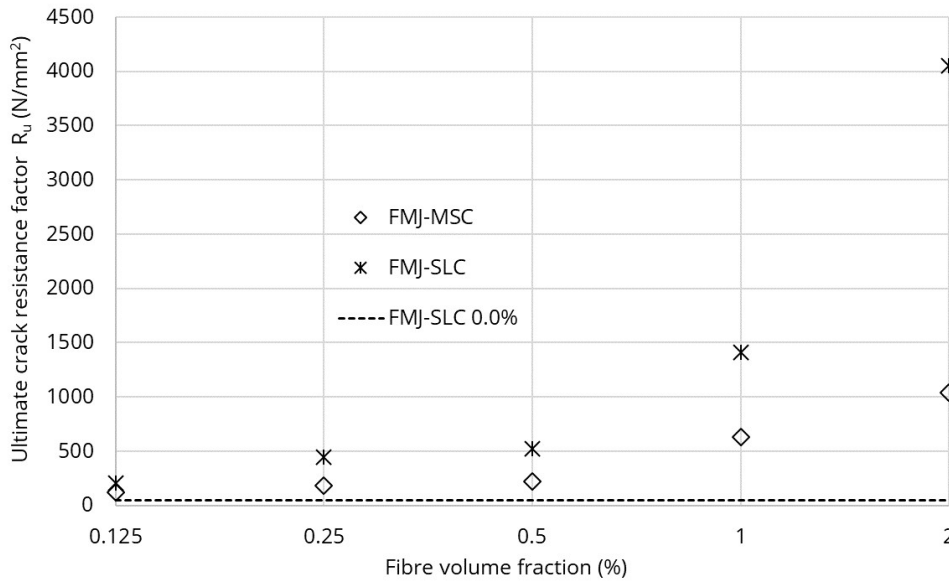


FIGURE 5. Ultimate crack resistance factor vs. fibre volumetric fraction for both types of projectiles.

#### 4. CONCLUSIONS

In the experimental research, cube specimens made of the UHPFRC were subjected to a non-deformable and deformable projectile impact. Cubes were differentiated on the basis of the fibre volumetric content and effect of projectile impact was investigated in terms of the cratering damage. The aim of the experimental part was to describe the shape of the crater that was produced on the UHPFRC targets as a result of the deformable and non-deformable projectile impact. Based on the experimental results and statistical correlation analysis, the following conclusions can be drawn:

- (1.) An increase in the fibre volume fraction leads to an increase in mechanical properties. Compressive mechanical properties are far less affected by the fibre volumetric content than tensile and flexural mechanical properties.
- (2.) An increase in fibre volume fraction also provides an efficient solution for decreasing the intensity of shear crack propagation due to the deformable and non-deformable projectile impact.
- (3.) Statistical evaluation of the correlation between mechanical properties and main damage degrees emerged due to the rigid projectile impact showed that the depth of the penetration is more correlated to tensile and flexural strength than to unconfined compressive strength. However, the crater area and volume seem to be in a better correlation with the latter than with the former two.
- (4.) The conclusion that the DOP is more correlated to the tensile and flexural strength than the unconfined compressive strength is valid within the framework of this study and is attributed to the nature of the shallow penetration in these experiments.

- (5.) It should be noted that the compressive strength, tensile strength and flexural strength do not affect only the DOP and they should be taken with caution when standing alone. High-intensity triaxial stress state and the volume changes of concrete that occur during the penetration should also be taken into consideration.

#### ACKNOWLEDGEMENTS

This work was supported by the Ministry of Interior of the Czech Republic project VI20172020061. The authors also acknowledge the assistance from the technical staff at the Experimental Centre, Faculty of Civil Engineering, Czech Technical University in Prague; and students who participated in the project.

#### REFERENCES

- [1] Børvik T, Langseth M, Hopperstad OS, Polanco-Loria MA. Ballistic perforation resistance of high performance concrete slabs with different unconfined compressive strengths. Proc. first Int. Conf. high Perform. Struct. Compos. Sevilla, Spain WIT Press (ISBN 1-85312-904-6), 2002, p. 273–82.
- [2] Shirai T, Kambayashi A, Ohno T, Taniguchi H, Ueda M, Ishikawa N. Experiment and numerical simulation of double-layered RC plates under impact loadings. Nucl Eng Des 1997;176:195–205. doi:10.1016/S0029-5493(97)00142-8.
- [3] Ohno T, Uchida T, Matsumoto N, Takahashi Y. Local damage of reinforced concrete slabs by impact of deformable projectiles. Nucl Eng Des 1992;138:45–52. doi:10.1016/0029-5493(92)90277-3.
- [4] Kar AK. Residual velocity for projectiles. Nucl Eng Des 1979;53:87–95. doi:10.1016/0029-5493(79)90042-6.
- [5] Amde AM, Mirmiran A, A. Walter T. Local damage assessment of turbine missile impact on composite and multiple barriers. Nucl Eng Des 1997;178:145–56. doi:10.1016/S0029-5493(97)00206-9.

- [6] Riedel W, Nöldgen M, Straßburger E, Thoma K, Fehling E. Local damage to Ultra High Performance Concrete structures caused by an impact of aircraft engine missiles. *Nucl Eng Des* 2010;240:2633–42. DOI:10.1016/J.NUCENGDES.2010.07.036.
- [7] Millon O, Riedel W, Mayrhofer C, Thoma K. Fiber-reinforced ultra-high performance concrete – a material with potential for protective structures. In: Li QM, Hao H, Li ZX, Yankelevsky D, editors. *Proc. First Int. Conf. Prot. Struct.*, Manchester: Manchester; 2010, p. no.-013.
- [8] Nicolaides D, Kanellopoulos A, Petrou M, Savva P, Mina A. Development of a new Ultra High Performance Fibre Reinforced Cementitious Composite (UHPFRCC) for impact and blast protection of structures. *Constr Build Mater* 2015;95:667–74. DOI:10.1016/j.conbuildmat.2015.07.136.
- [9] Bažantová Z, Kolář K, Konvalinka P, Litoš J. Multi-Functional High-performance Cement Based Composite. *Key Eng Mater* 2016;677:53–6. DOI:10.4028/www.scientific.net/KEM.677.53.
- [10] JSCE. Test method for bending strength and bending toughness of steel fiber reinforced concrete. *Standard Specification for Concrete Structures, Test Methods and Specifications*. 2005.
- [11] Banthia N, Majdzadeh F, Wu J, Bindiganavile V. Fiber synergy in Hybrid Fiber Reinforced Concrete (HyFRC) in flexure and direct shear. *Cem Concr Compos* 2014;48:91–7. DOI:10.1016/j.cemconcomp.2013.10.018.
- [12] Sovják R, Shanbhag D, Konrád P, Zatloukal J. Response of Thin UHPFRC Targets with Various Fibre Volume Fractions to Deformable Projectile Impact. *Procedia Eng.*, vol. 193, 2017, p. 3–10. DOI:10.1016/j.proeng.2017.06.179.
- [13] Wille K, El-Tawil S, Naaman AE. Properties of Strain Hardening Ultra High Performance Fiber Reinforced Concrete (UHP-FRC) under Direct Tensile Loading. *Cem Concr Compos* 2014. DOI:10.1016/j.cemconcomp.2013.12.015.
- [14] Sovják R, Vavříník T, Zatloukal J, Máca P, Mičunek T, Frydrýn M. Resistance of slim UHPFRC targets to projectile impact using in-service bullets. *Int J Impact Eng* 2015;76:166–77. DOI:10.1016/j.ijimpeng.2014.10.002.
- [15] Máca P, Sovják R, Konvalinka P. Mix design of UHPFRC and its response to projectile impact. *Int J Impact Eng* 2013;63:158–63. DOI:10.1016/j.ijimpeng.2013.08.003.
- [16] Li QM, Reid SR, Wen HM, Telford AR. Local impact effects of hard missiles on concrete targets. *Int J Impact Eng* 2005;32:224–84. DOI:10.1016/j.ijimpeng.2005.04.005.
- [17] Kneubuehl BP, Sellier KG. *Wound ballistics. Basics Appl Heidelberg* 2011.
- [18] Kankam CK. Impact Resistance of palm kernel fibre-reinforced concrete pavement slab. *J Ferrocem* 1999;29(4):279–86.
- [19] Alhasanat MBA, Al Qadi AN. Impact behavior of high strength concrete slabs with pozzolana as coarse aggregate. *Am J Appl Sci* 2016;13:754–61. DOI:10.3844/ajassp.2016.754.761.
- [20] Yankelevsky DZ. Resistance of a concrete target to penetration of a rigid projectile - revisited. *Int J Impact Eng* 2017;106:30–43. DOI:10.1016/j.ijimpeng.2017.02.021.
- [21] Kong X, Fang Q, Wu H, Peng Y. Numerical predictions of cratering and scabbing in concrete slabs subjected to projectile impact using a modified version of HJC material model. *Int J Impact Eng* 2016;95:61–71. DOI:10.1016/J.IJIMPENG.2016.04.014.